Extract of *Codiaeum luzonicum* Merr. overcomes multidrug resistance in human colon cancer cells by modulating *P*−glycoprotein

Regina Joyce E. Ferrer[✉], Marc Justin C. Ong, Sonia D. Jacinto

Institute of Biology, University of the Philippines Diliman, Quezon City, Metro Manila, Philippines

ABSTRACT

Objective: To investigate anti-multidrug resistance (MDR) activity and safety of the bioactive fraction (CL11) from *Codiaeum luzonicum* crude leaf extract.

Methods: Cytotoxic activity of CL11 against MDR and non-resistant colon cancer cells was assessed using MTT assay. Mode of cell death was investigated by annexin V-propidium iodide staining, TUNEL, and JC-1 assays. To examine mechanism of action, the effect on the expression and function of the MDR-implicated protein *P*-glycoprotein was tested using Western blotting and calcein assay, respectively.

Results: CL11 had an EC_{50} of 0.18, 1.03 and 38.52 µg/mL against HCT-15, HCT-15/Dox and HCT116, respectively. Cytotoxicity was mediated by inhibition of *P*-glycoprotein function and expression. The mode of cell death involved mitochondrial membrane depolarization and was mostly non-apoptotic at EC_{50} concentrations against HCT-15 and HCT-15/Dox.

Conclusions: Fraction CL11 of *Codiaeum luzonicum* induces non-apoptotic cell death in MDR cancer cells by overcoming MDR through inhibition of *P*-glycoprotein expression and function.

KEYWORDS: Natural product; Leaf extract; *Codiaeum luzonicum*; MDR cancer; *P*-gp inhibitor; Colorectal cancer

1. Introduction

Cancer is a leading cause of illness and death worldwide, with the latest global statistics indicating 19.3 million new cases and 10 million cancer-related deaths in 2020[1]. Despite significant advances in anticancer drug development, morbidity and mortality have been steadily rising in recent years. A major cause of treatment failure is resistance to the drugs administered[2]. Tumor cells may develop resistance to several anticancer drugs that are mechanistically and structurally unrelated[3]. This phenomenon is termed multidrug resistance (MDR). A common mechanism involves the ABC transport protein *P*-glycoprotein (*P*-gp) that increases drug efflux in the tumor cell membrane[4], leading to sublethal intracellular drug concentrations. *P*-gp expression has been identified as a marker of chemoresistance and decreased survival in various cancers[5]. Therefore, there is a strong need for research towards the development of treatments that can overcome MDR cancer, potentially by targeting *P*-gp.

Plants are a good source of such therapeutic candidates. Many drugs of plant origin are part of the standard repertory of anticancer chemotherapy[6]. Among these are vinblastine and vincristine from *Catharanthus roseus*, and etoposide and teniposide, which are semi-synthetic derivatives from *Podophyllum peltatum*[7]. In addition, many phytochemicals have been discovered or modified to bypass

---

Significance

Multidrug resistance is a major cause of failure in cancer chemotherapy. This study revealed that the fraction CL11 of *Codiaeum luzonicum* overcomes multidrug resistance by inhibiting the expression and function of the membrane pump *P*-glycoprotein, and kills multidrug-resistant cancer cells *via* induction of mitochondrial depolarization and non-apoptotic cell death. CL11 also exhibits low cytotoxicity against normal cells and therefore selectively kills cancer cells.

[✉]To whom correspondence may be addressed. E-mail: referrer@up.edu.ph

P-gp-mediated efflux; such as camptothecins from *Camptotheca acuminata*[8]. Some phytochemicals have been found to exploit *P*-gp, such as verapamil, a synthetic analog of a compound from *Papaver somniferum* that loses its cytotoxic activity against cancer cell lines that do not overexpress *P*-gp[8]. Other phytochemicals overcome MDR by lowering *P*-gp expression. This type of activity has been reported for curcumin[9], quercetin[10,11], and kaempferol[10].

Screening for candidate therapeutics from plants used in traditional medicine is a good strategy; persistence of the medicinal use of these plants throughout several generations prognosticates bioactivity and precludes toxicity. One plant that is a potential source of new anti-MDR cancer drugs is *Codiaeum luzonicum* (*C. luzonicum*) Merr. It is a Philippine endemic plant under the family Euphorbiaceae, belonging to the same genus as the globally popular ornamental plant *Codiaeum variegatum* or garden croton[12]. It grows in primary forests at low elevation and exhibits a patchy distribution within the country[13]. Indigenous communities in the Philippines use it to treat stomachaches[14] and ailments locally called binat[15]–described as a general unpleasant condition following pregnancy, which may include fever, fatigue, and/or malaise. Despite this, the only published study on its bioactivity was a biochemical systematics study on Euphorbiaceae which screened for phorbol ester bioactivity and reported the presence of phorbol esters in the 50:50 methylene chloride-methanol crude extract of *C. luzonicum*[16]. In a study using cancer cell lines, we found that the leaf extract of *C. luzonicum* was cytotoxic against the MDR cell line HCT-15. Therefore, in this study, we aimed to investigate the anti-MDR activity and safety of this *C. luzonicum* extract.

2. Materials and methods

2.1. Plant material

Leaves of *C. luzonicum* were collected from Mt. Lamao, Bataan, Philippines. Sample identification was authenticated at the Jose Vera Santos Memorial Herbarium, University of the Philippines, Diliman, Quezon City where a voucher specimen was deposited (Accession No. 18648).

2.2. Preparation of C. luzonicum extracts

Collected leaves were washed with tap water, oven-dried, and ground into fine powder. A crude extract was prepared by soaking the powdered leaves in 90% methanol for 3 d. The leaf suspension was filtered and then concentrated by rotary evaporation to obtain 20.6 g of crude extract (5.27% yield). This extract was then subjected to exhaustive solvent partitioning to obtain 5.1 g of hexane partition (1.3% yield), 4.6 g of ethyl acetate partition (1.2% yield), and 8.2 g of aqueous partition (2.1% yield).

Bioactivity-guided extraction was performed to isolate the active leaf fraction. Results of the MTT assay against MDR cell line HCT-15 were used as a basis for bioactivity. Hexane partition was the most cytotoxic and was therefore selected for VLC fractionation. To do this, the hexane partition was dry-loaded into a Merck silica gel 60 column at a 1:50 ratio. Fractions from the extract were eluted with hexane-ethyl acetate gradients from 100% hexane to 100% ethyl acetate at 10% increments, followed by 1:1 ethyl acetate-ethanol, and then 100% ethanol. Eluate from each solvent mixture was collected as one fraction. Among the VLC fractions, CL11 (eluted with 100% ethyl acetate) was chosen for further testing as it exhibited the best cytotoxic activity. The percent yield of CL11, however, was one of the lowest among fractions at 0.05%.

A stock solution of 20 mg CL11 in 1 mL DMSO was prepared for subsequent assays.

2.3. Cell lines and antibodies

Human colorectal cancer cell lines HCT-15 and HCT116, mouse embryo fibroblast cell line NIH/3T3, and human neonatal dermal fibroblast cell line HDFn were purchased from the American Type Culture Collection (ATCC, Manassas, VA, USA). The MDR cell line HCT-15/Dox was established by continuous sublethal exposure of HCT-15 to doxorubicin. The anti-*P*-gp mouse monoclonal antibody C219 was purchased from Calbiochem-Merck (Darmstadt, Germany), catalog number 517310.

2.4. Maintenance of cell cultures

All cell culture reagents used were purchased from Gibco-Thermo Fisher Scientific (Waltham, MA, USA). HCT116, HCT-15, HCT-15/Dox and NIH/3T3 cells were cultured as described previously[17]. HDFn was cultured in Dulbecco's Modified Eagle Medium supplemented with 10% fetal calf serum and 10 µL gentamicin per 100 mL culture medium. All cells were incubated at 37 ℃ in a 5% CO_2 atmosphere and passaged at 80%-95% confluency using a 0.05% trypsin-EDTA solution.

2.5. Evaluation of cytotoxic activity and selectivity using MTT assay

MTT assay was performed as described previously[17]. HCT116, HCT-15, and HCT-15/Dox were seeded at a density of 7 600 cells/well, and NIH/3T3 and HDFn were at a density of 11 400 cells/well in a 96-well plate. Absorbance reading was performed using a Varioskan Flash spectral scanning multimode reader (Thermo Scientific-Thermo Fisher Scientific, Waltham, MA, USA). A widely used chemotherapeutic drug, doxorubicin was used as the positive control, while dimethyl sulfoxide (DMSO) served as the negative control. Percent inhibition was calculated per treated well using the

formula: (Absorbance$_{DMSO}$ − Absorbance$_{treatment}$)/Absorbance$_{DMSO}$ × 100.

EC_{50} was then calculated from a percent inhibition *vs.* log of concentration plot using the software Graphpad Prism. Eight concentrations optimized for fitting a sigmoidal dose-response curve were tested per cell line. At least three independent experiments were performed in triplicate wells.

2.6. Detection of apoptosis using TUNEL assay

HCT116, HCT-15, and HCT-15/Dox cells were seeded in a 96-well plate as described in the MTT assay. Cells were treated with EC_{50} concentrations of CL11 and corresponding DMSO dilutions. After 72 h of incubation, cells were fixed with 4% paraformaldehyde and permeabilized with 0.25% Triton X-100. Positive control wells were treated with DNase Ⅰ just before TUNEL staining. The Click-iT® TUNEL Alexa Fluor® Imaging Kit (Invitrogen-Thermo Fisher Scientific, Waltham, MA, USA) was used according to the manufacturer's instructions with slight modifications. Cells were counterstained with nuclear stain Hoechst 33342 and washed twice with 1×PBS before microscopic examination using an inverted fluorescent microscope Axiovert.A1 (Carl Zeiss Microscopy GmbH, Jena, Germany) at 400× magnification. Images of the cells were obtained using Axiocam ICm1 (Carl Zeiss Microscopy GmbH, Jena, Germany). Colors were assigned as Alexa Fluor® 488 (green) and Hoechst (blue). Three independent experiments were conducted in duplicates, where five fields of view were observed per replicate.

2.7. Detection of apoptosis using annexin V−propidium iodide (PI) assay

HCT116, HCT-15, and HCT-15/Dox cells were seeded in a 96-well plate as described in MTT assay. After 24 h, the cells were treated with CL11, DMSO, or 2 μM of paclitaxel (positive control). EC_{50} concentrations of CL11 and corresponding DMSO dilutions for each cell line were used. After 24 h of incubation with the treatments, apoptotic cells were identified using Alexa Fluor® 488 Annexin V/Dead Cell Apoptosis Kit (Invitrogen-Thermo Fisher Scientific, Waltham, MA, USA). To prepare for staining, the plates were centrifuged for 5 min at 400 ×g and 22 ℃, then the supernatant was carefully removed by pipetting, and wells were washed twice with 1× annexin binding buffer. Then, 50 μL of 1× annexin-binding buffer, and 2 μL of a 1:5 solution of PI and Alexa Fluor® 488-annexin V solution from the kit were added to each well. After a 15-minute incubation at 37 ℃ in the dark, cells were washed once with 1× annexin binding buffer before microscopic examination using Axiovert.A1. Images of the cells were also obtained using Axiocam ICm1. Colors were assigned as Alexa Fluor® 488 (green) and PI (red). The assay was performed once in duplicate, where five

fields of view were observed per replicate.

2.8. Evaluation of changes in mitochondrial membrane potential (ΔΨm) using JC−1 assay

HCT116, HCT-15, and HCT-15/Dox cells were seeded in 96-well plates as described in MTT assay. After 24 h, cells were treated with 3 μg/mL CL11 or an equivalent dilution of DMSO for 72 h. ΔΨm was evaluated using the Mitoprobe JC-1 Assay Kit (Invitrogen-Thermo Fisher Scientific, Waltham, MA, USA) based on the manufacturer's instructions. Positive control carbonyl cyanide 3-chlorophenylhydrazone (CCCP) was added to corresponding wells following JC-1 incubation. Red fluorescence was measured at excitation/emission: 535/595 nm, while green fluorescence was measured at excitation/emission: 485/535 nm using Varioskan Flash. Two independent experiments were performed in triplicates.

2.9. Evaluation of P−gp expression using Western blotting assay

A total of 800 000 HCT-15 cells were seeded into 60 mm culture dishes. After 24 h, dishes were left untreated, or treated with DMSO, and 30 μg/mL, 3 μg/mL, 0.3 μg/mL, and 0.03 μg/mL CL11. Following 72 h of treatment, whole-cell lysates were extracted using RIPA buffer (supplemented with 1 M dithiothreitol, 2 mg/mL leupeptin, and 0.2 M phenylmethylsulfonyl fluoride). Proteins were separated from cell debris by centrifugation for 10 min at 15 000 rpm and 4 ℃. Total protein concentrations of the lysates were determined through Bradford assay using bovine serum albumin as a standard.

Protein samples were incubated at room temperature for 1 h before loading 20 μL of 6 μg protein per well of an SDS-PAGE gel. The 10-250 kDa Precision Plus Protein® All Blue prestained protein ladder (Bio-Rad Laboratories, Inc., Hercules, CA, USA) and the 10-220 kDa Benchmark® unstained protein ladder (Life Technologies-Thermo Fisher Scientific, Waltham, MA, USA) were used as molecular weight standards. A 7% acrylamide separating gel was used. Proteins were separated *via* electrophoresis using 500 V and 20 mA for the stacking gel, and 500 V and 30 mA for the separating gel. Afterward, protein bands were transferred to a nitrocellulose membrane using a semi-dry blotter (2 mA/cm², 25 V, 105 min). After the transfer, the membrane was blocked with 5% skimmed milk in 1× Tris-buffered saline supplemented with 0.05% Tween 20 (TBST) for 1 h at room temperature in a horizontal shaker. After blocking, the membrane was laminated in a clear plastic folder and cut at the 50 kDa level. The upper half of the membrane was incubated with a 1:1 000 dilution of the C219 anti-*P*-gp antibody, while the lower half was incubated with a 1:10 000 dilution of an anti-actin antibody. Both were incubated overnight at 4 ℃. On the second day, membranes were incubated with a 1:5 000 dilution of the HRP-

conjugated goat anti-mouse secondary antibody at room temperature for 1 h. Amersham ECL Western Blotting Detection reagent (GE Healthcare, Buckinghamshire, UK) was used to visualize the protein bands. The luminescence signal was developed on film. Bands were measured using the software ImageJ. *P*-gp measurements were normalized to actin band measurements.

2.10. Evaluation of P–gp activity using the calcein AM assay

Calcein assay was performed based on the kit manufacturer's instructions with some modifications (Molecular Probes, Eugene, OR, USA). Inhibition of *P*-gp function may be *via* direct interaction with *P*-gp, in which case the effect is immediate, or *via* affecting signaling relevant to *P*-gp function (indirect), in which case the effect will take longer.

To test CL11 activity as a direct inhibitor of *P*-gp function, HCT-15 and HCT-15/Dox cells were seeded at 5000 cells per well in a white, opaque 96-well plate. The cells were treated with 0.03, 0.3 and 3 µg/mL CL11, an equivalent dilution of DMSO, or 5 µg/mL of verapamil (positive control) 24 h after seeding. Cells were incubated at 37℃ with the treatments for 30 min, before the addition of calcein.

To test CL11 activity as an indirect inhibitor of *P*-gp function, HCT-15, and HCT-15/Dox cells were seeded at 7600 cells per well in a white opaque 96-well plate. After 24 h, the cells were treated with CL11, DMSO, or verapamil, as mentioned above. Cells were incubated under standard culture conditions for 72 h before addition of calcein.

For both set-ups, 50 µL of 2.5 µM calcein AM was added per well. Intracellular calcein retention was measured (excitation/emission: 494/517 nm) 45 min after addition of calcein.

2.11. Detection of P–gp in the colon cancer cell lines using immunocytochemistry

HCT116, HCT-15 and HCT-15/Dox cells were seeded in a black optical bottom 96-well plate as described in MTT assay. After 24 h, the culture medium was carefully removed by pipetting and cells were washed twice with 1×PBS. Cells were then fixed with 4% formaldehyde for 20 min on ice. Afterwards, cells were washed three times with 1×PBS and then permeabilized with 0.2% Triton-X-100 for 10 min at room temperature. Cells were again washed three times with 1×PBS before blocking each well with 100 µL 5% FBS in 1×PBS for 1 h at room temperature. The plate was placed in an orbital shaker at 20 rpm during the incubation period. Next, cells were washed twice with 1×PBS and then incubated with 30 µL of a 2 µg/mL (1:36) dilution of the primary antibody (in 5% FBS in 1×PBS) overnight at 4℃. On the second day, cells were washed twice with 1×PBS and then incubated with an Alexa fluor® 488-conjugated donkey anti-mouse antibody for 1 h at room temperature. Afterwards, cells were again washed twice and counterstained with DAPI by adding 50 µL of a 1 µg/mL solution per well. Following a 5-minute incubation, cells were washed twice with 1×PBS, before dispensing a final volume of 50 µL 1×PBS per well. Microscopic examination was performed using an inverted fluorescent microscope Axiovert.A1 (Carl Zeiss Microscopy GmbH, Jena, Germany) at 400× magnification. Images of the cells were obtained using a monochromatic camera Axiocam ICm1 (Carl Zeiss Microscopy GmbH, Jena, Germany). Colors were assigned as *P*-gp (green) and DAPI (blue). The assay was performed once in triplicate.

2.12. Statistical analysis

Statistical analyses were conducted in R[18]. Western blot data, where values ranged from 0-1, were analyzed using a beta regression Tukey's multiple comparisons test using the packages "betareg"[19], "emmeans"[20], and "multcompView"[21]. For the rest of the data, ANOVA followed by Tukey's multiple comparisons test was used to compare groups. Distribution of residuals was determined using the package "fitdistrplus"[22].

3. Results

3.1. Cytotoxic activity of CL11

CL11 was highly cytotoxic against HCT-15 and HCT-15/Dox with mean EC_{50} values of 0.180 µg/mL and 1.033 µg/mL, respectively (Supplementary Table 1). Furthermore, CL11 was significantly more cytotoxic than the control drug doxorubicin (Figure 1) for HCT-15 and HCT-15/Dox. While doxorubicin's cytotoxic effect decreased with increasing resistance, CL11 was significantly more cytotoxic against MDR cells than the non-MDR HCT116 (Figure 1). These results demonstrate the potent cytotoxic activity of CL11 against MDR cancer cells.

It was also interesting to note that CL11 exhibited poor cytotoxicity against HCT 116, with a mean EC_{50} value of 38.520 µg/mL (Supplementary Table 1), despite HCT 116 also being an epithelial colon cancer cell line like HCT-15 and HCT-15/Dox. This indicated a specific mechanism of action that targets MDR.

3.2. Safety and selectivity of CL11

CL11 exhibited selective cytotoxicity against MDR tumor cells and minimal toxicity against normal cells (Figure 2), as indicated by its high EC_{50} values against normal fibroblast cell lines NIH/3T3 and HDFn (Supplementary Table 1). The difference between CL11's EC_{50} against NIH/3T3 or HDFn, and its EC_{50} against either HCT-15/Dox or HCT-15 was highly significant ($P < 0.001$, Tukey's HSD). CL11 was also less cytotoxic to NIH/3T3 than the chemotherapeutic drug doxorubicin ($P < 0.001$; Supplementary Figure 1). EC_{50} values of CL11 against NIH/3T3 and HDFn were comparable to that against HCT116 (Supplementary Table 1). Overall, these results indicate safety and good selectivity of CL11 in killing cancer cells over normal cells.
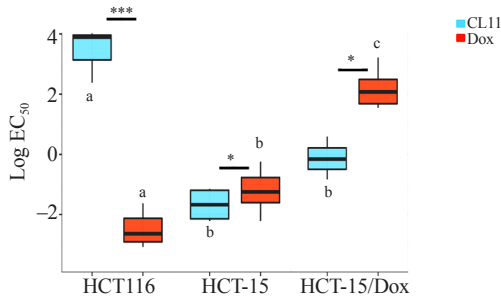
Figure 1. EC_{50} of CL11 for multidrug resistant (MDR) cancer cells HCT-15/Dox and non-MDR cancer cells HCT-15 and HCT116. Cells were treated with eight concentrations of CL11 or doxorubicin (Dox). Cytotoxic activity was assessed using MTT assay 72 h after treatment. EC_{50} values were computed based on nonlinear regression of percent inhibition versus log concentration graph using the software Graphpad Prism. The center line of the boxplot indicates the median value, the lower and upper hinges represent the 25th and 75th percentiles or the minimum and maximum points, and the whiskers denote $1.5\times$ the interquartile range. Data represent at least three independent trials performed in triplicate wells. Letters represent significant differences based on one-way ANOVA with Tukey's multiple comparisons test that compared EC_{50} across cell lines for each treatment ($P < 0.05$). *$P < 0.05$; ***$P < 0.001$, one-way ANOVA.
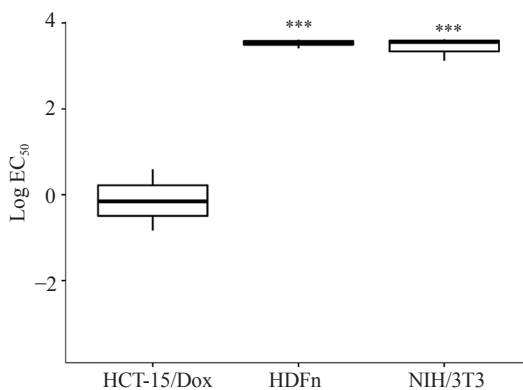
Figure 2. Safety and selectivity of CL11. CL11 shows significantly less cytotoxicity against normal fibroblast cells compared to MDR cancer cells. HCT-15/Dox, HDFn, and NIH/3T3 cells were treated with eight concentrations of CL11. Cytotoxic activity was assessed using MTT assay 72 h after treatment. EC_{50} values were computed based on nonlinear regression of percent inhibition versus log concentration graph using the software Graphpad Prism. The center line of the boxplot indicates the median value, the lower and upper hinges represent the 25th and 75th percentiles or the minimum and maximum points, and the whiskers denote $1.5\times$ the interquartile range. Data represent at least three independent experiments performed in triplicate wells. Asterisks indicate statistical difference compared with the results in HCT-15/Dox; ***$P < 0.001$, one-way ANOVA with Tukey's multiple comparisons test.

3.3. Mode of cell death induced by CL11

TUNEL assay that detects late apoptosis by staining breaks in the DNA strand and annexin V-PI assay that detects early apoptosis by staining externalized phosphatidylserine were performed to determine if CL11 induces cell death *via* the apoptotic pathway.

Results of the TUNEL assay indicate that the mode of cell death induced by CL11 was mainly apoptotic in HCT116. On the other hand, the main mode of cell death was non-apoptotic in HCT-15 and HCT-15/Dox as indicated by the very small fraction of TUNEL-stained nuclei (Figures 3A-B). In addition, enlarged nuclei were observed in CL11-treated HCT-15 and HCT-15/Dox cells but not in CL11-treated HCT116 cells (indicated by red arrowheads in Figures 3A-B). This difference in morphology supports different modes of cell death induced between non-MDR and MDR colon cancer cells.

Results of the annexin V-PI assay coincided with those of the TUNEL assay. For this assay, early apoptotic cells would only exhibit green fluorescence. Of the three cell lines, only HCT116 had cells that only stained green (Figure 4C); for HCT-15 and HCT-15/Dox, stained cells were positive for both annexin V and PI (Figures 4A-B). It has also been observed that for HCT-15 and HCT-15/Dox, green fluorescence was present in both the cell membrane and the cytoplasm (Figures 4A-B). Positive PI staining together with annexin V staining in the cytoplasm indicated that the plasma membrane was already disintegrating; a phenomenon that does not occur until the late stages of apoptosis but occurs at the onset of necrosis. This was also observed in paclitaxel-treated HCT-15 and HCT-15/Dox cells, albeit to a lesser extent. Annexin V fluorescence in HCT116, on the other hand, appeared to be localized in the cell membrane (Figure 4C); as was expected given that annexin V labels phosphatidylserine which localizes to the outer leaflet of the plasma membrane during apoptosis.

### 3.4. Effect of CL11 on mitochondrial membrane potential

CL11 induced a loss of $\Delta\Psi$m in HCT116 and HCT-15 cells (Figure 5), indicating that its cytotoxic activity was mediated by mitochondrial depolarization. In HCT-15/Dox, the effect of CL11 (and CCCP) was likely masked by the effect of *P*-gp; given that *P*-gp can pump out JC-1, and HCT-15/Dox had the highest *P*-gp expression among the three cell lines (Supplementary Figure 2). This coincided with the trend in mitochondrial membrane potentials of the cell lines, where it was highest in HCT116 and lowest in HCT-15/Dox ($P < 0.001$). The same trend was observed for both red and green raw fluorescence readings.

3.5. Effect of CL11 on P−gp expression

Based on preceding results that indicated a strong cytotoxic activity of CL11 which appeared specific to MDR cells, we investigated whether the mechanism for this bioactivity was related to *P*-gp, a common mechanism for resistance in cancer cells.

A

B

C
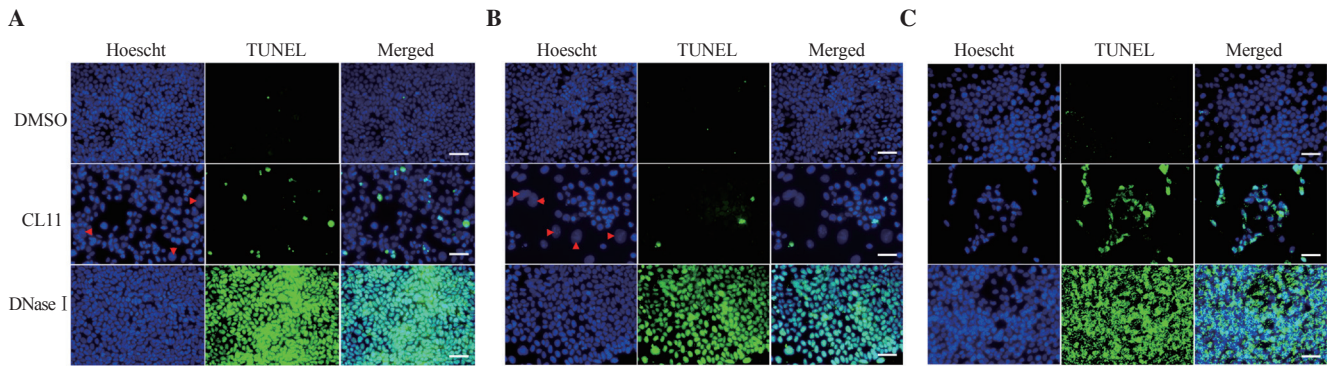
Figure 3. Cells were treated with EC$_{50}$ concentration of CL11. DMSO served as the negative control, while DNase Ⅰ served as the positive control. Apoptosis was detected using TUNEL staining 72 h after treatment. Cells were counterstained with the nuclear stain Hoechst. Red arrowheads indicate enlarged nuclei. Photographs were taken at a magnification of 400× and represent five fields of view from three trials performed in duplicate wells. (A) HCT-15, (B) HCT-15/Dox, (C) HCT116. Scale bar, 100 μm.

A

B

C
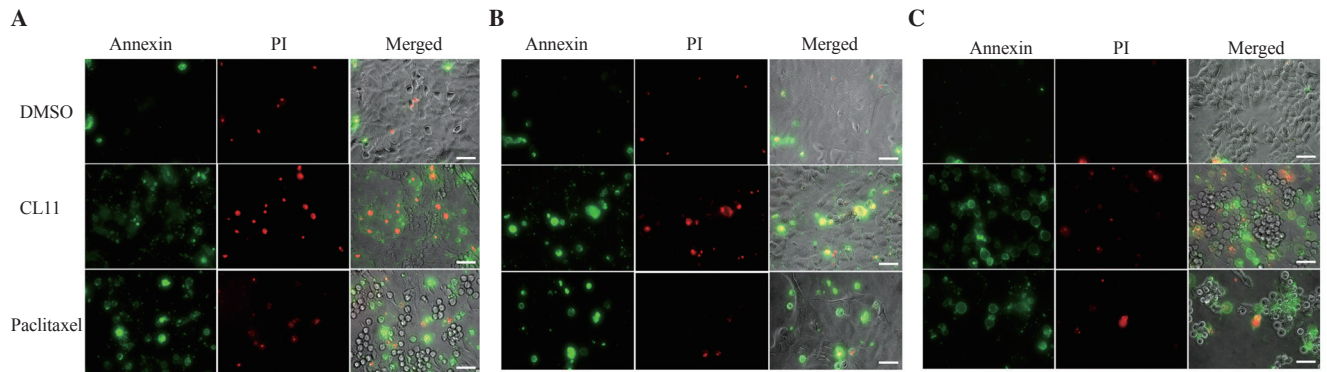
Figure 4. Cells were treated with EC$_{50}$ concentration of CL11. DMSO served as the negative control, while 2 μM paclitaxel served as the positive control. Apoptosis was detected using annexin-V-PI staining 24 h after treatment. Photographs were taken at a magnification of 400× and represent five fields of view from one trial performed in duplicate wells. (A) HCT-15, (B) HCT-15/Dox, (C) HCT116. Scale bar, 100 μm.

Western blotting results indicated that treatment with CL11 for 72 h reduced *P*-gp expression in HCT-15 cells. The response observed was biphasic: 3 μg/mL CL11 elicited the most significant downregulation of percent *P*-gp at 75.9% ($P < 0.001$) (Supplementary Table 2). Moreover, 30 μg/mL CL11 elicited a lower percent *P*-gp downregulation than 0.3 μg/mL at 61.1% *vs.* 66.6% (Figure 6). *P*-gp downregulation by 0.03 μg/mL was 49.4% but was not statistically significant ($P = 0.077$).

3.6. Effect of CL11 on P−gp function

We also determined whether the effect of CL11 on *P*-gp expression translates to an effect on *P*-gp function. CL11 treatment for 72 h increased calcein fluorescence in both HCT-15 and HCT-15/Dox (Figure 7). Consistent with the Western blotting results, inhibition of calcein efflux following 72-h treatment was significant ($P < 0.001$) at concentrations above 0.3 μg/mL (Figure 7). On the other hand, CL11 treatment for 30 min did not increase calcein fluorescence in HCT-15 or HCT-15/Dox (Figure 7).

These results indicate that CL11 was not a direct (*e.g.* competitive inhibitor) inhibitor of *P*-gp. On the other hand, long-term exposure to CL11 improved cellular retention of calcein, which is a substrate of *P*-gp.
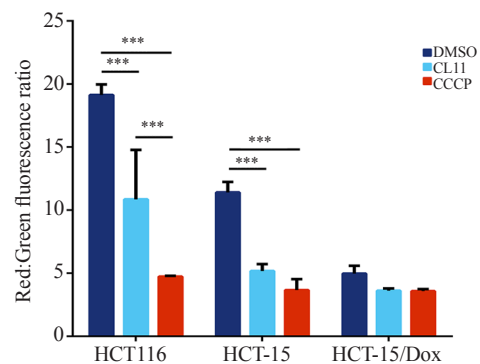
Figure 5. CL11 induces loss of mitochondrial membrane potential in HCT116 and HCT-15. HCT116, HCT-15, and HCT-15-Dox cells were treated with 3 μg/mL CL11. DMSO served as the negative control, while carbonyl cyanide 3-chlorophenylhydrazone (CCCP) served as the positive control. ΔΨm was measured *via* JC-1 staining 72 h after treatment. High red to green fluorescence ratio corresponds to a high ΔΨm. Data are expressed as mean ± SE of two independent experiments performed in triplicate wells. [***]$P < 0.001$, ANOVA with Tukey's multiple comparisons test.
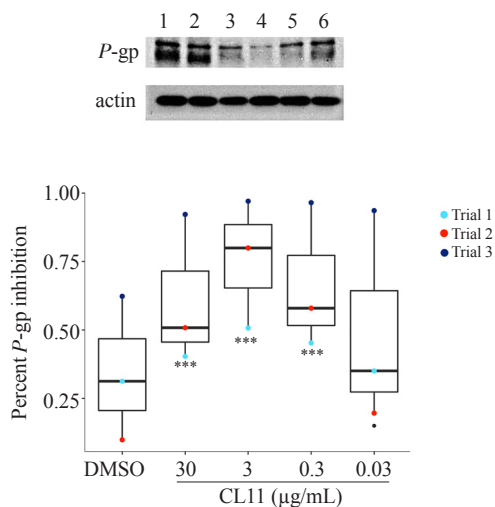
Figure 6. CL11 downregulates *P*-gp expression in a biphasic manner in Western blotting assay. *P*-gp (150-170 KDa) was identified using the C219 monoclonal mouse antibody. Actin was used as loading control. The amount of *P*-gp was calculated from densitometric analysis of *P*-gp bands normalized to actin bands. Western blot lanes 1-6: no treatment, DMSO, 30 μg/mL CL11, 3 μg/mL CL11, 0.3 μg/mL CL11, 0.03 μg/mL CL11. The center line of the boxplot indicates the median value, the lower and upper hinges represent the 25th and 75th percentiles or the minimum and maximum points, and the whiskers denote 1.5× the interquartile range. Asterisks indicate statistical differences compared with DMSO. $^{*}P = 0.077$; $^{***}P < 0.001$, two-way beta regression with Tukey's multiple comparisons test.

4. Discussion

Natural products are an important source of anticancer drugs; 31.46% of all drugs used to treat cancer from the 1940s to 2019 are natural products or derivatives thereof[23]. Plants, in particular, contribute significantly to the roster of natural product anticancer drugs and are an important source of many standard anticancer drugs such as vincristine, etoposide, and topotecan.

In the present study, a VLC fraction (CL11) from *C. luzonicum*,

a Philippine endemic plant used in traditional medicine, was investigated for its anti-MDR activity. The bioactivity of *C. luzonicum* is practically unexplored. There is only one other published bioactivity study for this plant[16], which only reports the presence of phorbol esters in the crude extract that competitively inhibited dibutyrate binding to protein kinase C. Leaf extracts from this plant were specifically chosen for this study because of their promising results in our previous anticancer bioactivity screens. In particular, bioactivity assays were performed on VLC fraction CL11 because anticancer activity appeared to diminish upon further purification.

To assess the cytotoxic activity of CL11, three colorectal cancer cell lines were used: HCT-15, HCT-15/Dox, and HCT116. HCT-15 expresses high levels of *P*-gp[24–26] and is more resistant to MDR-associated drugs than non-MDR drugs[24,26]. Despite these, however, HCT-15 is not commonly used as a model for studies in multidrug-resistant cancer and is not specified as MDR by ATCC, from where the cell line was procured. Thus, we established an MDR subline of HCT-15 (HCT-15/Dox) through constant exposure to sublethal doses of doxorubicin[27]. *P*-gp expression of HCT-15/Dox is twice that of HCT-15, and it is 7-82 times more resistant to anticancer drugs than HCT-15 (unpublished data). Another colorectal cancer cell line, HCT116 exhibits no difference in cytotoxicity between MDR and non-MDR drugs and has low or no *P*-gp expression[26,28]. Based on these, HCT116 is taken to be non-MDR, HCT-15 as intermediately-MDR, and HCT-15/Dox as highly MDR. Results of this study show that CL11 is highly cytotoxic against HCT-15 and HCT-15/Dox. Its EC$_{50}$ against both cell lines was significantly lower than the chemotherapeutic drug doxorubicin. CL11, however, exhibited poor cytotoxicity against non-MDR colon cancer cell line HCT116, toward which doxorubicin was most cytotoxic. For doxorubicin, this pattern of cytotoxic activity could be explained by the fact that it is an MDR-associated drug, and is a substrate of the efflux action of *P*-gp[26,27]. For CL11, these results may indicate that its mechanism of action specifically targets MDR cells. CL11's poor cytotoxic activity against non-cancer cells (EC$_{50}$ comparable to
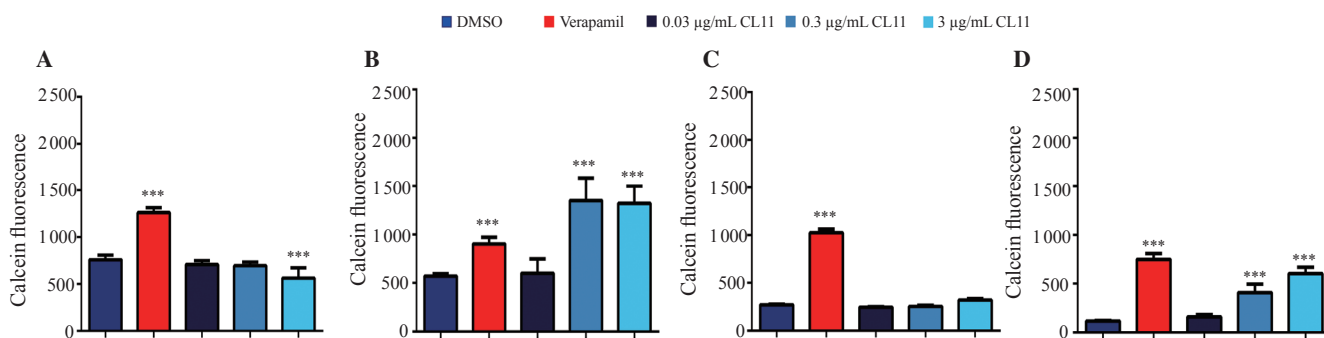
Figure 7. CL11 inhibits *P*-gp function after long-term exposure (72 h). HCT-15 (A: 30 min; B: 72 h) and HCT-15/Dox (C: 30 min; D: 72 h) cells were treated with different concentrations of CL11. DMSO served as the negative control, while verapamil served as the positive control. Calcein fluorescence was measured after 30 min or 72 h of treatment and served as a measure of *P*-gp activity. Data are expressed as mean ± SE of three independent experiments performed in triplicate wells. Asterisks indicate statistical differences compared with DMSO. $^{***}P < 0.001$, ANOVA with Tukey's multiple comparisons test.

that against HCT116) also supports this hypothesis. Additional tests are, however, needed to confirm if CL11's target is not related to another characteristic exclusive to HCT-15 and its subline HCT-15/Dox. This can be done by testing CL11 toxicity on additional MDR cell lines, including at least one more MDR colorectal cancer cell line. Still, many compounds are known to overcome cancer MDR by exploiting *P*-gp. Examples include verapamil, cytosine arabinoside, gemcitabine[29], and thiosemicarbazones[30]. These compounds show preferential activity toward MDR cancer cells relative to their non-MDR parental cells; a phenomenon termed collateral sensitivity[29]. A proposed mechanism of action for such compounds is the generation of reactive oxygen species (ROS)[8,31].

Taken together, results of annexin V-PI and TUNEL staining indicate that the main mode of cell death induced by CL11 was apoptotic in HCT116 cells, and non-apoptotic in HCT-15 and HCT-15/Dox cells. This dual mechanism of cell death has also been reported for the synthetic indole compound BPR0L075[32]. BPR0L075 induced apoptosis in non-MDR ovarian cancer cell lines OVCAR-3 and SKOV-3. Meanwhile, in paclitaxel-resistant sublines of OVCAR-3 and SKOV-3, cell death was primarily due to mitotic catastrophe. These results coincide with the findings that *P*-gp inhibits apoptosis by modulating the expression of apoptosis proteins[33,34]. In one study, inhibition of radiation-induced apoptosis by *P*-gp overexpression occurred simultaneously with increases in radiation-induced mitotic catastrophe and senescence[35]. The observed enlargement of nuclei, as well as the positive staining for both annexin V and PI in CL11-treated HCT-15 and HCT-15/Dox, correspond with the findings of Eom *et al.*[36] on mitotic catastrophe accompanied by a senescence-like phenotype. In their study, they found doxorubicin-induced apoptosis at high doses and mitotic catastrophe at low doses. In our study, the HCT116 cells that underwent apoptosis were also treated with a much higher dose of CL11 for the annexin V-PI and TUNEL assays because we used the EC$_{50}$ concentrations of CL11 for each cell line. Further experiments are needed to determine whether the different modes of cell death exhibited by CL11 are an effect of different mechanisms of action against HCT116 versus against HCT15 and HCT15/Dox, an effect of differences in *P*-gp expression, or an effect of the dose administered – such as the case in doxorubicin[36]. The mode of cell death induced by CL11 can also be better characterized through flow cytometry analysis of annexin V-PI cells, and determination of markers of specific cell death pathways.

We also investigated whether CL11 causes depolarization of the mitochondrial membrane as a possible mechanism for inducing cell death. CL11 induced depolarization of the mitochondrial membrane in both HCT-15 and HCT116 cells. Mitochondrial depolarization facilitates cytochrome c release, which can in turn initiate caspase activation in apoptosis[37]. However, it is also associated with necrosis[38] and mitotic catastrophe[39], which eventually leads to

apoptosis or necrosis. It can also precede or occur in parallel with senescence[36,40]. The lack of significant depolarization in HCT-15/Dox is likely due to *P*-gp pumping out significant amounts of the indicator dye JC-1[41].

Given CL11's strong cytotoxic activity against MDR cells that diminishes in non-MDR and non-cancer cells, as well as the varying modes of cell death induced by CL11 in non-MDR versus in MDR cancer cells, we next investigated the effect of CL11 on *P*-gp expression and function. Overexpression of *P*-gp and other membrane efflux pumps is a common mechanism for drug resistance in cancers[42]. *P*-gp can mediate the efflux of a very wide range of substrates including several commonly used chemotherapeutic agents[43]. Its expression in tumors is often correlated with poor patient prognosis[29,42].

In previous decades, there has been a lot of interest in the development of *P*-gp inhibitors to overcome MDR in cancer chemotherapy. However, there is still no MDR inhibitor approved for clinical use to date[4]. Reasons for failing to pass clinical trials included inconsistent or insignificant efficacy, negative impacts on anticancer drug pharmacokinetics, and unacceptable toxicity[29,42]. The lack of success in clinical trials resulted in an almost complete shutdown of studies in the field. Further clinical trials using *P*-gp inhibitors were vehemently discouraged[42]. Yet, drug resistance remains a significant problem in cancer treatment, and *P*-gp expression in clinical samples continues to be correlated with poor treatment outcomes.

Our Western blotting results indicate that treatment with CL11 for 72 h reduced *P*-gp expression in a biphasic manner. While it is common for *P*-gp to exhibit a biphasic response to inhibitors, low doses often stimulate *P*-gp function while high doses inhibit it *i.e.* U-shaped curve[44]. We have found no reports of cases such as in this study where a high dose enhances *P*-gp expression while low doses inhibit it. Interestingly, the induction of apoptosis by the *P*-gp-exploiting drug verapamil exhibits the same biphasic trend[31]. Verapamil induced maximum cell death at 10 μM, followed by improved cell survival at 50 μM. Upon elucidation of verapamil's mechanism of action, it was found that it activates *P*-gp ATPase with the same biphasic trend, inducing maximal activation at 10 μM as well. The elevated ATP demand resulting from activated ATPase causes increased oxidative phosphorylation that would in turn produce ROS as by-products. These ROS deplete cellular glutathione, ultimately leading to apoptosis. Regarding *P*-gp expression, low levels of ROS downregulate its expression, while high levels of ROS result in an upregulation of expression[45,46]. The mechanism of action of CL11 may involve ROS production, thereby explaining the biphasic response observed in Western blotting assay. Moreover, ROS can cause DNA damage, leading to mitotic catastrophe[47], as well as trigger opening of the mitochondrial membrane transition pores necessary for necrosis[48]. Results of

the calcein assay show that CL11 induced an increase in calcein fluorescence on HCT-15 and HCT-15/Dox cells after 72 h of treatment but elicited no effect after 30 min of treatment. Together, Western blotting and calcein assay results indicate that CL11 is not a direct inhibitor of *P*-gp but it decreases *P*-gp function after prolonged treatment by downregulating *P*-gp expression. This is interesting because *P*-gp inhibitors are often screened or designed based on their binding to *P*-gp, making most of them direct inhibitors. Direct inhibitors can be competitive or non-competitive inhibitors. Competitive inhibitors exert their function by tightly binding and blocking the substrate binding sites, while non-competitive inhibitors bind to a non-substrate binding site and consequently inhibit ATPase activity or modulate *P*-gp function allosterically[29]. CL11 elicits its function in neither way. Its modulation of *P*-gp expression may be through targeting a molecule upstream of *P*-gp, by interacting with the *P*-gp promoter, or by modulating ROS signaling, as discussed earlier. The specific mechanism can be elucidated in future studies.

Numerous studies suggest that compounds modulating cellular ROS levels can sensitize MDR cancer cells to chemotherapeutic drugs and enhance MDR cancer cell death[49]. Further, reports of increased ROS levels and scavenging/antioxidant enzyme activity in MDR cancer cells compared to non-MDR cancer and normal cells indicate that MDR cancer cells are particularly more susceptible to alterations in ROS levels[49]. This hypothesis can be further explored for CL11's mechanism of action in future studies.

Overall, the results of this study indicate that fraction CL11 of *C. luzonicum* induces mostly non-apoptotic cell death in MDR cancer cells by overcoming MDR through inhibition of *P*-gp expression and function. CL11 also shows significant selectivity against cancer cells over normal cells, and a specific mechanism of action as opposed to being generally toxic. By being able to both kill cancer cells and inhibit *P*-gp at the same time, CL11 may circumvent the difficulties associated with the co-administration of a *P*-gp inhibitor and a separate chemotherapeutic drug. Previously encountered difficulties include varying pharmacokinetic properties and additive toxicities. CL11 also presents a different mechanism of inhibiting *P*-gp from previously developed inhibitors that failed in the clinical trials; it downregulates *P*-gp expression as opposed to binding to the protein to directly interfere with *P*-gp action.

In subsequent studies, elucidation of the specific extract components will be another important contribution to the scientific literature on this plant. Such data will also support potential drug development and the discovery of new bioactivities from *C. luzonicum*.

In addition to colorectal cancer, significant *P*-gp expression has also been reported in liver cancer, lung cancer, breast cancer, gastric cancer, osteosarcoma, prostatic cancer, and renal cancer[43]. High expression of *P*-gp has also been reported in cancer stem cells, which are known to play a key role in cancer progression and recurrence[43]. Therefore, CL11's cytotoxic activity against other cancer cells that overexpress *P*-gp could be further explored in future studies.

Conflict of interest statement

The authors declare that there is no conflict of interest.

Authors' contributions

RJEF designed the methodology and data analysis, performed the experiments and data analysis, and drafted and revised the manuscript. MJCO performed the experiments and data analysis for assessing extract safety. SDJ acquired funding for the project, supervised the project and contributed to the final version of the manuscript.

References

[1] Sung H, Ferlay J, Siegel RL, Laversanne M, Soerjomataram I, Jemal A, et al. Global cancer statistics 2020: GLOBOCAN estimates of incidence and

mortality worldwide for 36 cancers in 185 countries. *CA Cancer J Clin* 2021; **71**(3): 209-249.

[2] Vasan N, Baselga J, Hyman DM. A view on drug resistance in cancer. *Nature* 2019; **575**(7782): 299-309.

[3] Wu Q, Yang Z, Nie Y, Shi Y, Fan D. Multi-drug resistance in cancer chemotherapeutics: Mechanisms and lab approaches. *Cancer Lett* 2014; **347**(2): 159-166.

[4] Zhang H, Xu H, Ashby CR, Assaraf YG, Chen Z, Liu H. Chemical molecular-based approach to overcome multidrug resistance in cancer by targeting *P*-glycoprotein (*P*-gp). *Med Res Rev* 2021; **41**(1): 525-555.

[5] Bradley G, Ling V. *P*-glycoprotein, multidrug resistance and tumor progression. *Cancer Metastasis Rev* 1994; **13**(2): 223-233.

[6] Becker C, Hoffmann K, Hoffmann L, King T, Faulstich F, Viertel K, et al. Established anticancer drugs from natural origin. In: Kuete V, Efferth T (eds.) *Biodiversity, natural products and cancer treatment.* 1st ed. Toh Tuck Link, Singapore: World Scientific Publishing Co Pte Ltd; 2014, p. 343-389.

[7] Kuete V, Efferth T. *Biodiversity, natural products and cancer treatment.* Toh Tuck Link, Singapore: World Scientific Publishing Co. Pte. Ltd.; 2014.

[8] Nobili S, Landini I, Mazzeu T, Mini E. Overcoming tumor multidrug resistance using drugs able to evade *P*-glycoprotein or to exploit its expression. *Med Res Rev* 2012; **32**(6): 1220-1262.

[9] Lopes-Rodrigues V, Sousa E, Vasconcelos MH. Curcumin as a modulator of *P*-glycoprotein in cancer: Challenges and perspectives. *Pharmaceuticals* 2016; **9**(4): 71-81.

[10] Limtrakul O, Khantamat K, Pintha P. Inhibition of *P*-glycoprotein function and expression by kaempferol and quercetin. *J Chemother* 2005; **17**(1): 86-95.

[11] Li S, Zhao Q, Wang B, Yuan S, Wang X, Li K. Quercetin reversed MDR in breast cancer cells through down-regulating *P*-gp expression and eliminating cancer stem cells mediated by YB-1 nuclear translocation. *Phyther Res* 2018; **32**(8): 1530-1536.

[12] Cordero-Ramos N, Ventosa-Febles EA. *Codiaeum variegatum* (garden croton). [Online]. Invasive Species Compendium; 2017. Available from: https://www.cabi.org/isc/datasheet/11858#tosummaryOfInvasiveness [Accessed on April 6 2022].

[13] Pelser PB, Barcelona JF, Nickrent DL. Euphorbiaceae. [Online]. Co's Digital Flora of the Philippines. 2017. Available from: https://www.philippineplants.org/Families/Euphorbiaceae.html [Accessed on April 6 2022].

[14] Johnson T. *Ethnobotany desk reference*. Boca Raton: CRC Press; 1999.

[15] Canceran ML, Henric Gojo Cruz PP, Abella EA, Castillo DC, Gandalera EE, Judan Cruz KG. Ethnomedicinal plants of the Dumagat community of Paraiso, Culat, Casiguran, Aurora, Philippines. *Int J Biosci* 2021; **18**(3): 261-267.

[16] Beutler JA, Alvarado AB, McCloud TG, Cragg GM. Distribution of phorbol ester bioactivity in the Euphorbiacea. *Phyther Res* 1989; **3**(5): 188-192.

[17] Dante RAS, Ferrer RJE, Jacinto SD. Leaf extracts from *Dillenia philippinensis* rolfe exhibit cytotoxic activity to both drug-sensitive and multidrug-resistant cancer cells. *Asian Pacific J Cancer Prev* 2019; **20**(11): 3285-3290.

[18] "R Core Team." R: A language and environment for statistical computing. [Online]. Vienna, Austria: R Foundation for Statistical Computing; 2019. Available from: https://www.r-project.org/ [Accessed on December 6 2021].

[19] Cribari-Neto F, Zeileis A. Beta regression in R. *J Stat Softw* 2010; **34**(2): 1-24.

[20] Lenth R. emmeans: Estimated Marginal Means, aka Least-Squares Means. [Online]. Available from: https://cran.r-project.org/package=emmeans [Accessed on December 6 2021].

[21] Graves S, Piepho HP, Selzer L, Dorai-Raj S. multcompView: Visualizations of Paired Comparisons. [Online]. Available from: https://cran.r-project.org/package=multcompView [Accessed on December 6 2021].

[22] Delignette-Muller ML, Dutang C. fitdistrplus: An R Package for Fitting Distributions. *J Stat Softw* 2015; **64**(4): 1-34.

[23] Newman DJ, Cragg GM. Natural products as sources of new drugs over the nearly four decades from 01/1981 to 09/2019. *J Nat Prod* 2020; **83**(3): 770-803.

[24] Izquierdo MA, Shoemaker RH, Flens MJ, Scheffer GL, Wu L, Prather TR, et al. Overlapping phenotypes of multidrug resistance among panels of human cancer-cell lines. *Int J Cancer* 1996; **65**(2): 230-237.

[25] Stein U, Walther W, Shoemaker RH. Reversal of multidrug resistance by transduction of cytokine genes into human colon carcinoma cells. *J Natl Cancer Inst* 1996; **88**(19): 1383-1392.

[26] Wu L, Smythe AM, Stinson SF, Mullendore LA, Monks A, Scudiero DA, et al. Multidrug-resistant phenotype of disease-oriented panels of human tumor cell lines used for anticancer drug screening multidrug-resistant phenotype of disease-oriented panels of human tumor cell lines used for anticancer drug screening. *Cancer Res* 1992; **52**(11): 3029-3034.

[27] Uchiyama-Kokubu N, Watanabe T. Establishment and characterization of adriamycin-resistant human colorectal adenocarcinoma HCT-15 cell lines with multidrug resistance. *Anticancer Drugs* 2001; **12**(9): 769-779.

[28] Stein U, Walther W, Shoemaker R. Modulation of mdr1 expression by cytokines in human colon carcinoma cells: An approach for reversal of multidrug resistance. *Br J Cancer* 1996; **74**(9): 1384-1391.

[29] Jaramillo AC, Saig F Al, Cloos J, Jansen G, Peters GJ. How to overcome ATP-binding cassette drug efflux transporter-mediated drug resistance? *Cancer Drug Resist* 2018; **1**(1): 6-29.

[30] Hall MD, Salam NK, Hellawell JL, Fales HM, Kensler CB, Ludwig JA, et al. Synthesis, activity, and pharmacophore development for isatin-β-thiosemicarbazones with selective activity toward multidrug-resistant cells. *J Med Chem* 2009; **52**(10): 3191-3204.

[31] Karwatsky J, Lincoln MC, Georges E. A mechanism for *P*-glycoprotein-mediated apoptosis as revealed by verapamil hypersensitivity. *Biochemistry* 2003; **42**(42): 12163-12173.

[32] Wang X, Wu E, Wu J, Wang TL, Hsieh HP, Liu X. An antimitotic and

antivascular agent BPR0L075 overcomes multidrug resistance and induces mitotic catastrophe in paclitaxel-resistant ovarian cancer cells. *PLoS One* 2013; **8**(6): e65686.

[33]Souza PS, Madigan JP, Gillet JP, Kapoor K, Ambudkar SV, Maia RC, et al. Expression of the multidrug transporter *P*-glycoprotein is inversely related to that of apoptosis-associated endogenous TRAIL. *Exp Cell Res* 2015; **336**(2): 318-328.

[34]Shman TV, Fedasenka UU, Savitski VP, Aleinikova OV. CD34+ leukemic subpopulation predominantly displays lower spontaneous apoptosis and has higher expression levels of *Bcl–2* and *MDR1* genes than CD34- cells in childhood AML. *Ann Hematol* 2008; **87**(5): 353-360.

[35]Ruth AC, Roninson IB. Effects of the multidrug transporter *P*-glycoprotein on cellular responses to ionizing radiation. *Cancer Res* 2000; **60**(10): 2576-2578.

[36]Eom YW, Kim MA, Park SS, Goo MJ, Kwon HJ, Sohn S, et al. Two distinct modes of cell death induced by doxorubicin: apoptosis and cell death through mitotic catastrophe accompanied by senescence-like phenotype. *Oncogene* 2005; **24**(30): 4765-4777.

[37]Gottlieb E, Armour S, Harris M, Thompson C. Mitochondrial membrane potential regulates matrix configuration and cytochrome c release during apoptosis. *Cell Death Differ* 2003; **10**: 709-717.

[38]Halestrap A. A pore way to die. *Nature* 2005; **434**(7033): 578-579.

[39]Castedo M, Perfettini JL, Roumier T, Valent A, Raslova H, Yakushijin K, et al. Mitotic catastrophe constitutes a special case of apoptosis whose suppression entails aneuploidy. *Oncogene* 2004; **23**(25): 4362-4370.

[40]Vitale I, Galluzzi L, Castedo M, Kroemer G. Mitotic catastrophe: A mechanism for avoiding genomic instability. *Nat Rev Mol Cell Biol* 2011; **12**(6): 385-392.

[41]Kühnel J, Perrot J, Faussat A, Marie J, Schwaller M. Functional assay of multidrug resistant cells using JC-1, a carbocyanine fluorescent probe. *Leukemia* 1997; **11**: 1147-1155.

[42]Robey RW, Pluchino KM, Hall MD, Fojo AT, Bates SE, Gottesman MM. Revisiting the role of ABC transporters in multidrug-resistant cancer. *Nat Rev Cancer* 2018; **18**(7): 452-464.

[43]Nobili S, Lapucci A, Landini I, Coronnello M, Roviello G, Mini E. Role of ATP-binding cassette transporters in cancer initiation and progression. *Semin Cancer Biol* 2020; **60**: 72-95.

[44]Calabrese EJ. *P*-glycoprotein efflux transporter activity often displays biphasic dose-response relationships. *Crit Rev Toxicol* 2008; **38**(5): 473-487.

[45]Felix RA, Barrand MA. *P*-glycoprotein expression in rat brain endothelial cells: Evidence for regulation by transient oxidative stress. *J Neurochem* 2002; **80**(1): 64-72.

[46]Wartenberg M, Ling FC, Schallenberg M, Bäumer AT, Petrat K, Hescheler J, et al. Down-regulation of intrinsic *P*-glycoprotein expression in multicellular prostate tumor spheroids by reactive oxygen species. *J Biol Chem* 2001; **276**(20): 17420-17428.

[47]Cornago M, Garcia-Alberich C, Blasco-Angulo N, Vall-llaura N, Nager M, Herreros J, et al. Histone deacetylase inhibitors promote glioma cell death by G_2 checkpoint abrogation leading to mitotic catastrophe. *Cell Death Dis* 2014; **5**(10): e1435.

[48]Kim JS, Jin Y, Lemasters JJ. Reactive oxygen species, but not Ca^{2+} overloading, trigger pH- and mitochondrial permeability transition-dependent death of adult rat myocytes after ischemia-reperfusion. *Am J Physiol Hear Circ Physiol* 2006; **290**(5): H2024-H2034.

[49]Cui Q, Wang JQ, Assaraf YG, Ren L, Gupta P, Wei L, et al. Modulating ROS to overcome multidrug resistance in cancer. *Drug Resist Updat* 2018; **41**: 1-25.